Modification of a Supported Lipid Bilayer by Polyelectrolyte Adsorption

Z. Vivian Feng, Steve Granick,* and Andrew A. Gewirth*

Department of Chemistry and Fredrick Seitz Materials Research Laboratory, University of Illinois at Urbana−Champaign, Urbana, Illinois 61801

Received April 16, 2004. In Final Form: July 13, 2004

Addition of a weak polyelectrolyte, poly(methacrylic acid) (PMA), to a supported phospholipid bilayer made from 1,2-dimyristoyl-*sn*-glycero-3-phosphocholine (DMPC) depresses the melting temperature and alters the morphology of the bilayer in the gel phase. Ellipsometry measurements show that PMA adsorption lowers the phase transition temperature by 2.4 °C. Atomic force microscopy (AFM) showed no visible contrast in the fluid phase (above the melting temperature) but a rich morphology in the gel phase. In the gel phase, adsorption leads to formation of significantly less mobile phospholipid islands and other defects. One consequence of this lower mobility is a decrease in the implied cooperativity number of the phase transition, *N*, when polymer is added. Additionally, AFM images of the gel-phase bilayer show a highly defected structure that anneals significantly more slowly than in the absence of adsorbed polymer. Tentatively, we suggest that PMA preferentially decorates island and defect edges of the DMPC bilayer.

1. Introduction

The interaction of macromolecules such as polymers and proteins with lipid membranes is important in areas as diverse as polymer science,[1,2] membrane biophysics,[3−5] and drug formulations.[6] There is considerable interest in using supported lipid bilayers as models for biophysical processes relevant to protein adsorption, drug formulation, vesicle formation, and sensing.[7,8] Detailed characterization of these supported bilayers both by themselves and upon incorporation of various materials can provide insight into the structure and reactivity of the bilayer film.

The most commonly used techniques for studying phase transitions in phospholipid bilayers are dynamic scanning calorimetry,[9] X-ray scattering,[10] and neutron reflectivity[11] measurements. However, these techniques are limited to studies of bilayer vesicles. For planar lipid bilayers on solid supports, the phase transition has been observed by using atomic force microscopy (AFM).[12−14] Ellipsometry is another technique that can monitor film thickness change as a function of temperature or other variables.

Poly(methacrylic acid) (PMA), a weak polyelectrolyte, shows strong dependence of the degree of dissociation on its local environment. The PMA−bilayer interaction acts as an easily tractable model for studying bilayer−macromolecule interactions. The time dependence of the adsorption of PMA onto a zwitterionic lipid bilayer has been recently examined.[15] Furthermore, poly(acrylic acid) derivatives have proven to be of particular interest in membrane studies because of their pH-dependent capacity to trigger changes in biophysical properties of lipid vesicles.[5,16,17]

One area of inquiry relates to the phase transition behavior of supported bilayer films. We showed recently that the fluid-to-gel phase transition engenders large defected areas in confined films supported on mica.[12] The origin of these defects was the increased density of the gel phase relative to fluid. From separate experimental approaches, an interesting perspective of the adsorption of PMA and its derivatives on lipid bilayers is their effect to increase the permeability of membranes. Previous work has postulated that PMA causes pore formation or stabilization.[5,16−18] However, there has been no direct examination of PMA interaction with bilayer membrane pores.

In this study, we focus on changes in the physical properties of a model lipid bilayer, 1,2-dimyristoyl-*sn*-glycero-3-phosphocholine (DMPC), induced by the adsorption of the weak polyelectrolyte, PMA. In particular, one of the most important physical properties of a lipid system is its gel−fluid phase transition behavior. We evaluate characteristics of the phase transition behavior, including the transition temperature and the transition cooperativity of the DMPC bilayer, under the influence of PMA adsorption. In addition, we examine the ability of PMA to stabilize defects in lipid bilayers. The experimental

* To whom correspondence should be addressed. A.A.G.: e-mail, agewirth@uiuc.edu; tel, 217-333-8329; fax, 217-333-2685. S.G.: e-mail, sgranick@uiuc.edu; tel, 217-333-5720; fax, 217-244-2278.

(1) Savva, M.; Torchilin, V. P.; Huang, L. *J. Colloid Interface Sci.* **1999**, *217*, 160−165.
(2) Savva, M.; Torchilin, V. P.; Huang, L. *J. Colloid Interface Sci.* **1999**, *217*, 166−171.
(3) Shai, Y. *Biochim. Biophys. Acta* **1999**, *1462*, 55−70.
(4) Eum, K. M.; Langley, K. H.; Tirrell, D. A. *Macromolecules* **1989**, *22*, 2755−2760.
(5) Thomas, J. L.; Tirrell, D. A. *J. Controlled Release* **2000**, *67*, 203−209.
(6) Mayer, L. D.; Krishna, R.; Webb, M.; Bally, M. *J. Liposome Res.* **2000**, *10*, 99−115.
(7) Sackmann, E. *Science* **1996**, *271*, 43−48.
(8) Dufrene, Y. F.; Lee, G. U. *Biochim. Biophys. Acta* **2000**, *1509*.
(9) Lewis, R. N. A. H.; Mak, N.; McElhaney, R. N. *Biochemistry* **1987**, *26*, 6118−6126.
(10) Tristram-Nagle, S.; Liu, Y.; Legleiter, J.; Nagle, J. F. *Biophys. J.* **2002**, *83*, 3324−3335.
(11) Johnson, S. J.; Baryerl, T. M.; McDermott, D. C.; Adam, G. W.; Rennie, A. R.; Thomas, R. K.; Sackmann, E. *Biophys. J.* **1991**, *59*, 289−294.
(12) Xie, A. F.; Yamada, R.; Gewirth, A. A.; Granick, S. *Phys. Rev. Lett.* **2002**, *89*, 246103.
(13) Tokumasu, F.; Jin, A. J.; Dvorak, J. A. *J. Electron Microsc.* **2002**, *51*, 1−9.
(14) Tokumasu, F.; Jin, A. J.; Feigenson, G. W.; Dvorak, J. A. *Ultramicroscopy* **2003**, *97*, 217−227.
(15) Xie, A. F.; Granick, S. *Nat. Mater.* **2002**, *1*, 129−133.
(16) Seki, K.; Tirrell, D. A. *Macromolecules* **1984**, *17*, 1692−1698.
(17) Mourad, P. D.; Murphy, N.; Porter, T. M.; Poliachik, S. L.; Crum, L. A.; Hoffman, A. S.; Stayton, P. S. *Macromolecules* **2001**, *34*, 2400−2401.
(18) Thomas, J. L.; Tirrell, D. A. *Acc. Chem. Res.* **1992**, *25*, 336−342.

10.1021/la049030w CCC: $27.50
Published on Web 09/02/2004

conditions in this study were selected to parallel those of another recent study, in which, using methods of Fourier transform infrared (FTIR) spectroscopy, polyelectrolyte-induced surface reconstruction of DMPC bilayers was also investigated.[15]

2. Experimental Section

2.1. Sample Preparation. 2.1.1. Materials. All solutions were prepared with ultrapure water (Milli-Q UV plus, Millipore Inc., 18.2 MΩ cm). A 10 mM pH = 6.4 buffer was made from Na_2HPO_4 and $NaH_2PO_4 \cdot H_2O$ (PBS). The lipid, DMPC, was purchased from Avanti Polar Lipids, Inc. (Alabaster, AL) and used without further purification. The sodium salt of PMA was purchased from Polymer Standard Surface (Mainz, Germany) and used as received. The weight-average molecular weight of the PMA, M_w, was 40 000 g mol^{-1}, and the ratio of weight-average to number-average molecular weight, M_w/M_n, was 1.05. The concentration of the polymer solution was 0.1 mg/mL.

2.1.2. Si Substrate Preparation for Ellipsometry Measurements. Si wafers 0.76 mm thick were cut into 3.5 cm × 1.3 cm rectangles for use in the ellipsometry measurement. To generate a consistent thickness of SiO_2 on the Si substrate, the Si wafer was soaked in piranha bath for 1 h, followed by thorough rinsing with Millipore water. The wafer was then baked at 100 °C for 3 h to remove the water. Next, the wafer was placed in a UV−ozone cleaner for 30 min, followed by another 15 min of plasma cleaning. Finally, the Si substrate was stored in a clean vial filled with N_2. Using this preparation routine, highly hydrophilic surfaces (contact angle ≈ 0°) were achieved.

2.1.3. Lipid Bilayer Preparation. DMPC bilayers were prepared by using the vesicle fusion technique.[12] For AFM experiments, a sheet of freshly cleaved mica was used as a substrate and placed at the bottom of the AFM fluid cell. Lipid vesicles were injected in the cell and were incubated in a 45 °C oven for 1 h to encourage bilayer formation. Excess unfused vesicles were removed by exchanging the solution in the cell with buffer solution several times after cooling the sample to room temperature. AFM images of the pure (undecorated) bilayer agreed with those reported previously.[12]

In the experiments involving addition of PMA, 0.1 mg/mL PMA in PBS buffer was added to the preformed gel-phase DMPC bilayers and was allowed to adsorb for 4 min prior to rinsing. This short exposure time limited the coverage of PMA to ca. 5%.[15] The coverage of 5% was chosen because larger amounts of polymer were found to adsorb onto the AFM cantilever, resulting in the lipid peeling off of the mica during scanning. Following rinsing with fresh buffer solution to wash off unadsorbed PMA, the sample was again incubated at 45 °C for 1 h before imaging measurements. These polymer-"starved" systems reach equilibrium in approximately 4 h when the lipid bilayer is in the gel phase and within less than 1 h when lipids are in the fluid phase.[15]

For ellipsometry measurement, bilayers were formed on a pretreated Si wafer substrate. The Si substrate was secured by a metal clip against a stainless steel plate. The substrate was then placed in an optical cuvette and was three-quarter immersed in DMPC vesicle solution within the cuvette. The cuvette was incubated in a warm water bath at 45 °C for 1 h. Once the assembly was cooled to room temperature, the cuvette was flushed with a large amount of buffer solution to wash off unadsorbed vesicles. The entire cuvette and the cylindrical glass ellipsometry cell were immersed in a large buffer reservoir. Finally, the Si substrate was transferred into the ellipsometry cell from the cuvette while fully immersed in buffer. PMA was added to the system once the ellipsometry cell was fully assembled. In the case where PMA was allowed to fully adsorb on the bilayer, the cell was incubated at 45 °C for 1 h without further rinsing.

2.2. Magnetic Acoustic Mode (MAC) Atomic Force Microscopy. AFM experiments were carried out with a PicoSPM 300 (Molecular Imaging) with a Type D scanner controlled with a Nanoscope E controller (Digital Instruments). The cantilevers that we employed had a natural resonance frequency of 65−75 kHz in air and 22−25 kHz in the aqueous environment. The spring constant of the cantilever was 2.8 N/m. Images were collected at 256 × 256 pixel resolution at a scan rate of less than 2 Hz. Images were flattened with NanoScope E version 4.23 (Digital Instruments) and further analyzed by WSxM version 3.0 (Nanotec Electronica S. L.).

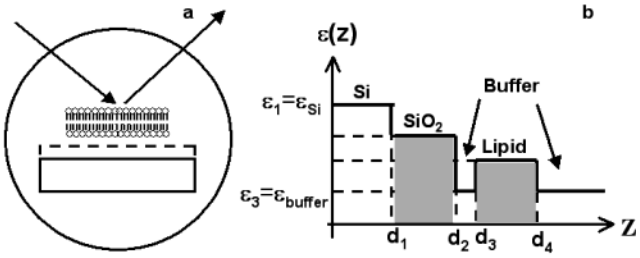

Figure 1. Top view of the ellipsometry cell with lipid bilayer adsorbed on treated Si substrate (a) and its dielectric profile (b). Integration of this plot gives information of the value measured (shadowed area).

Temperature control during the AFM experiment was realized by using the 1xPeltier sample stage (Molecular Imaging). The sample stage was wired to a Cryogenic Temperature Controlled, model DTC-500 (Lake Shore Cryogenic, Inc.), which provided heating current, and a home-built device that monitored the resistance of the RTD directly underneath the sample. An elevated ice−water reservoir using gravity feeding was used to cool the Peltier stage.

2.3. Phase-Modulated Ellipsometry. In situ ellipsometry measurements were obtained by using a home-built phase-modulated ellipsometer. The lipid bilayer sample on a Si substrate was positioned vertically in a cylindrical glass cell filled with buffer solution. A schematic top view of the cell is shown in Figure 1. A He−Ne laser beam was normally incident to the cell wall. The beam passed through the interfaces of buffer, lipid, thin water layer, SiO_2, and Si. Measurements at temperatures below room temperature were achieved by cooling the sample cell in a refrigerator before placing it in the test cell. Temperature control above room temperature was achieved using a heating mantle and a thermistor in a long-neck disposable pipet with the sealed end placed vertically in the cell close behind the Si substrate.

The ellipticity, $\bar{\rho}$, is very sensitive to surface structure at the Brewster angle and can be readily interpreted in terms of film thickness.[19,20] It is defined as the imaginary component of the complex reflection amplitude ratio for p- and s-polarized light at the Brewster angle. The relationship between $\bar{\rho}$ and the dielectric profile $\epsilon(Z)$ at depth Z is expressed by the Drude equation:

$$\bar{\rho} = \frac{\pi}{\lambda} \frac{\sqrt{\epsilon(-\infty) + \epsilon(+\infty)}}{\epsilon(-\infty) - \epsilon(+\infty)} \int_{-\infty}^{+\infty} \frac{[\epsilon(Z) - \epsilon(+\infty)][\epsilon(Z) + \mathrm{e}(-\infty)]}{\epsilon(Z)} \mathrm{d}Z \quad (1)$$

The dielectric profile in Figure 1 indicates the model for our system. Within this model, the Drude equation shows that $\bar{\rho}$ is directly proportional to the film thickness, L:

$$\bar{\rho} = \frac{\pi}{\lambda} \frac{\sqrt{\epsilon_{\mathrm{buffer}} + \epsilon_{\mathrm{Si}}}}{\epsilon_{\mathrm{buffer}} - \epsilon_{\mathrm{Si}}} \left[\frac{(\epsilon_{\mathrm{lipid}} - \epsilon_{\mathrm{buffer}})(\epsilon_{\mathrm{lipid}} - \epsilon_{\mathrm{Si}})}{\epsilon_{\mathrm{lipid}}} L + \frac{(\epsilon_{\mathrm{SiO_2}} - \epsilon_{\mathrm{buffer}})(\epsilon_{\mathrm{SiO_2}} - \epsilon_{\mathrm{Si}})}{\epsilon_{\mathrm{SiO_2}}} L_{\mathrm{SiO_2}} \right] \quad (2)$$

where $\epsilon_{\mathrm{buffer}} = 1.769$, $\epsilon_{\mathrm{Si}} = 15.07$, $\epsilon_{\mathrm{SiO_2}} = 2.123$,[19−21] and $\epsilon_{\mathrm{lipid}} = 2.103$.[22] ϵ values were calculated directly from n^2 (dielectric constant) values obtained from the literature. Usually, two pieces of Si wafers were prepared in parallel, one for lipid bilayer growth and the other as a calibration sample to confirm the SiO_2 layer thickness. The SiO_2 layer thickness was approximately 2 nm. In a typical ellipsometry measurement, eight $\bar{\rho}$ measurements were taken and averaged at a given temperature.

(19) Mukhopadhyay, A.; Law, B. M. *Phys. Rev. E* **2001**, *63*, 041605.
(20) Mukhopadhyay, A.; Law, B. M. *Phys. Rev. E* **2001**, *63*, 011507.
(21) Law, B. M.; Mukhopadhyay, A.; Henderson, J. R.; Wang, J. Y. *Langmuir* **2003**, *19*, 8380−8388.
(22) Puu, G.; Gustafson, I. *Biochim. Biophys. Acta* **1997**, *1327*, 149−161.

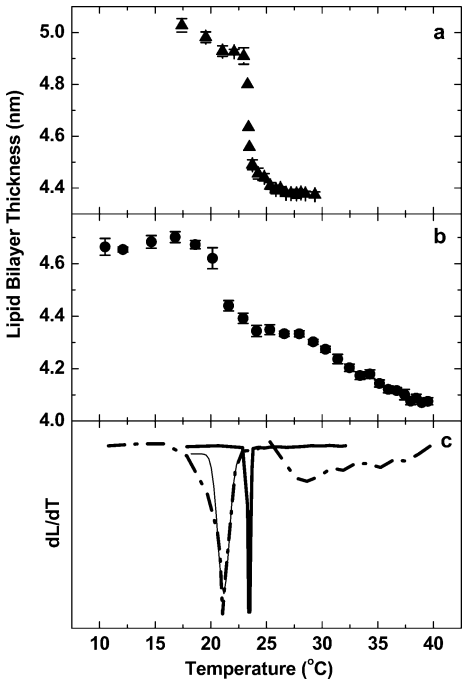

Figure 2. Phase-modulated ellipsometry as a function of temperature of (a) pure DMPC and (b) DMPC with excess PMA. (c) Differentiated thickness vs temperature curve for pure DMPC (solid line) and DMPC + PMA (dashed−dotted line). The thin solid line is a Gaussian fit for the DMPC + PMA data set.

3. Results

3.1. Phase-Modulated Ellipsometry. Using a phase-modulated ellipsometer, we measured the temperature dependence of the ellipticity, $\bar{\rho}$, of the DMPC bilayer on oxidized Si in both the gel and the fluid phases. The ellipticity is related to the film thickness, L, by using eq 2, and Figure 2 shows this thickness obtained as a function of temperature. The gel−fluid phase transition of the bilayer is manifested by an abrupt drop in film thickness. Previous spectroscopic ellipsometry,[22] quartz crystal microbalance-dissipation,[23,24] and measurements using other techniques have shown that the highly hydrophilic SiO_2 surface is an effective solid support for free-standing lipid bilayers prepared via the vesicle fusion procedure. The temperature coefficient of the refractive index for pure water is $1-2 \times 10^{-6}$ index unit per degree,[25] which is insignificant over the temperature range in which we worked. Therefore, this change was neglected in calculating the bilayer thickness.

The filled triangles in Figure 2a show that the pure DMPC bilayer was approximately 5.0 ± 0.1 nm thick, which is reasonable for a gel-phase DMPC bilayer.[11,26] The most striking feature of this curve is a sharp decrease in thickness at 23−24 °C. Before this sharp change, the thickness decreased moderately in the gel phase. Subsequently, it decreased continuously from 24 to 27 °C, until it leveled off beyond 27 °C at approximately 4.3 nm. Above 30 °C, the changes in thickness were insignificant (data not shown). The total change in thickness, 0.6 nm, is consistent with the height change expected between the gel and fluid phases of the DMPC bilayer. This measurement agrees well with our previous AFM study of the phase transition in DMPC bilayers[12] but is slightly larger than the value of 0.3−0.4 nm measured by neutron reflectivity.[11] The temperature at which this sharp transition occurs is exactly that expected for the main gel−fluid phase transition in pure DMPC.[9,27,28]

The circles in Figure 2b show the temperature dependence of the thickness obtained from an experiment in which 0.1 mg/mL PMA had been exposed to previously formed DMPC bilayers. Previous IR experiments have indicated an approximately 20% coverage when fluid-phase DMPC is exposed to such polymer solutions for up to 60 min (unpublished data). To ensure full coverage by PMA, excess polymer was retained in solution above the bilayer without further rinsing. Figure 2b shows that the initial thickness of the DMPC bilayer in the presence of polymer is 4.70 ± 0.05 nm. This value is 0.30 nm less than the thickness of the bare DMPC bilayer reported in Figure 2a.

Interestingly, the curve in Figure 2b looks quite different from that in Figure 2a. The sharp change in thickness takes place at a lower temperature than that found with pure DMPC. The slope of this decrease in thickness is also not as sharp as in the previous case. From 25 to 27 °C, the bilayer thickness did not change significantly after decreasing approximately 0.35 nm from the initial 4.70 nm. Beyond 27 °C, a further decrease in thickness takes place. This change is relatively less drastic, resulting in a total change of 0.25 nm over a 10 °C temperature range. No significant changes in bilayer thickness took place above 40 °C. The more rounded character of these changes, relative to those observed for undecorated DMPC bilayers, may indicate that polymer coverage of the surface was in some sense inhomogeneous, although we have no quantitative explanation at this time.

To better analyze the ellipsometry results, curves a and b of Figure 2 were differentiated, shown in Figure 2c. The solid line and the dashed−dotted line depict the cases of without and with PMA on the DMPC bilayer, respectively. The differentiated plots clearly indicate that there are two significant effects that PMA has on the DMPC bilayer phase transition: transition temperature and lipid cooperativity. The minima in the plots occur at 23.5 and 21.1 °C, respectively, allowing us to quantify that the DMPC gel-to-fluid phase transition temperature decreased by 2.4 °C upon adsorption of PMA. The ability of a substance to alter the phase transition characteristics of a lipid membrane reflects its association with the lipid. Additionally, analysis of the peak shape shows an almost factor of 5 increase (from 0.218 to 1.028 °C) in its full width at half-maximum (fwhm) when PMA was present. The peak width of this differentiated plot is closely related to the cooperativity of the lipid phase transition.[16,29] Finally, the dL/dT plot for the DMPC−PMA system is asymmetric. As shown in Figure 2c, a Gaussian fit to the DMPC−PMA dL/dT curve (thin solid line) reveals a substantial low-temperature tail. This tailing is not present in the system absent PMA.

3.2. AFM. The AFM studies presented below concern temperatures below the melting temperature, as no contrast was seen at higher temperatures.

3.2.1. Change in Morphology upon PMA Adsorption. To understand further the origin of the PMA-induced changes in the phase transition behavior, we performed

(23) Reimhult, E.; Hook, F.; Kasemo, B. *Phys. Rev. E* **2002**, *66*, 051905.
(24) Glasmastar, K.; Larsson, C.; Hook, F.; Kasemo, B. *J. Colloid Interface Sci.* **2002**, *146*, 40−47.
(25) Hawkes, J. B.; Astheimer, R. W. *J. Opt. Soc. Am.* **1948**, *38*, 804−806.
(26) Janiak, M. J.; Small, D. M.; Shipley, G. G. *Biochemistry* **1976**, *15*, 4575−4580.
(27) Marsh, D.; Watts, A.; Knowles, P. F. *Biochim. Biophys. Acta* **1977**, *465*, 500−514.
(28) Needham, D.; Evans, E. *Biochemistry* **1988**, *27*, 8261−8369.
(29) Borden, K. A.; Eum, K. M.; Langley, K. H.; Tirrell, D. A. *Macromolecules* **1987**, *20*, 454−456.

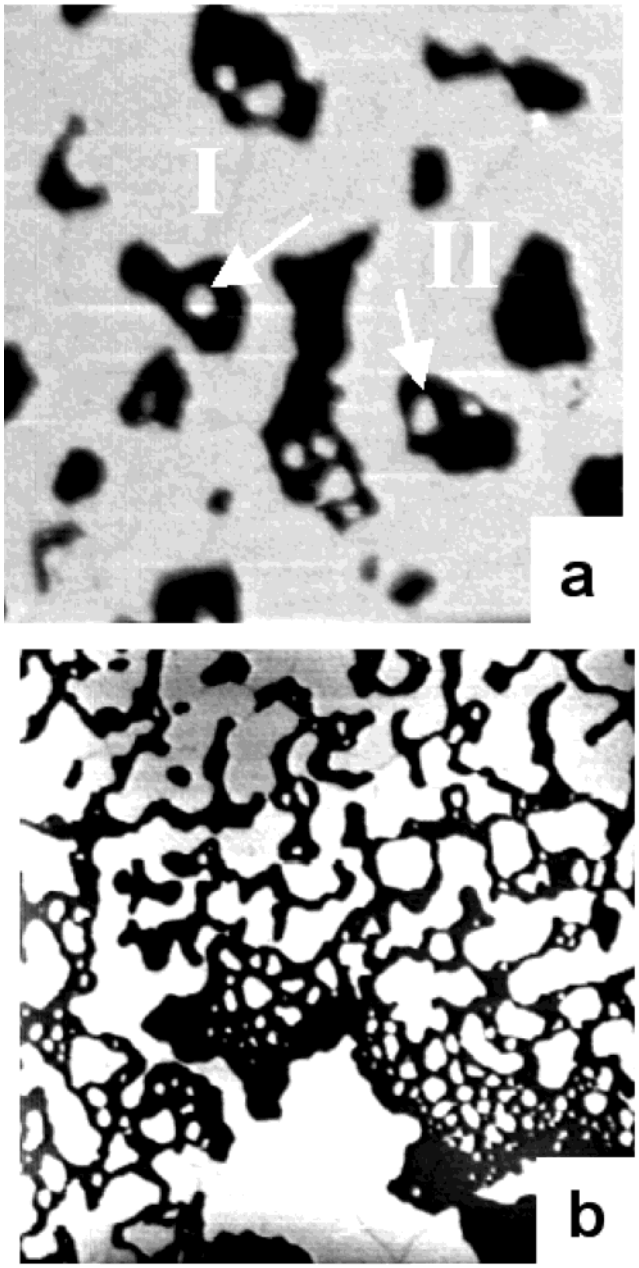

Figure 3. MAC-mode AFM images of gel-phase DMPC without (image a, $3 \times 3 \mu$m) and with (image b, $5 \times 5 \mu$m) PMA adsorption at 13 °C. Dark color is the mica substrate, and light color is the lipid bilayer.

AFM measurements examining the gel-phase DMPC bilayer. Figure 3a illustrates a typical AFM image of the gel-phase DMPC bilayer obtained at 13 °C. Homogeneously distributed defects in the bilayer were observed, as described previously.[12] The dark areas in the images are the underlying mica surface. In this image, the lipid bilayer coverage is approximately 80%. The origin of these defects is tearing of the bilayer as the density of the film decreases from that in the fluid phase to that in the gel phase in the constant volume AFM cell.[12] Slow cooling from fluid to gel phase while continuously monitoring the bilayer with AFM gives defects which are circular and more uniform than those reported here. Cross-section analysis of the defects in these images gives a bilayer thickness at this temperature of approximately 4.5 ± 0.3 nm, in good agreement with the DMPC bilayer thickness reported previously by techniques such as X-ray diffraction,[26] specular reflection of neutrons,[11] and AFM,[12−14] although slightly smaller than that obtained from ellipsometry.

In Figure 3a, lipid islands are observed inside the defects, two of which are marked with arrows. The diameters of these islands range from 90 to 170 nm. The formation of these features is attributed to the bilayer preparation procedure, which involves rapid cooling of bilayers from higher incubating temperature to lower temperature (13 °C).[12,30] The existence of these islands is associated with the limited time for lipids to migrate to the defect walls during cooling from the fluid phase. The island density is found to be considerably smaller following slow cooling from the fluid phase.

Figure 3b shows an AFM image of a DMPC bilayer on mica obtained at 13 °C following addition of PMA. There are several differences found between the PMA-free and PMA-modified systems.

First, the cracking pattern found with the PMA-modified DMPC bilayer appears as a series of channels rather than the oval defects found without PMA. The widths of the channels are remarkably uniform. Quantification of a random selection of 10 channels gave a line width with a magnitude of 148 ± 30 nm. Second, although the channel widths were uniform, AFM images of the PMA-modified system reveal considerable heterogeneity relative to the unmodified bilayer. Multiple AFM images showed that some areas are more heavily defected than others. Figure 3b shows an image obtained at the edge of a heavily defected area. In this selected area, the defect coverage was as high as 40%. Third, the image reveals numerous irregularly shaped lipid islands within the defected areas. The lipid islands exhibit a wide range of sizes, some of which were as small as 30 nm in diameter. However, the bilayer thickness was not affected by the presence of polymer. Cross-section analysis of the defects reveals the thickness to be 4.4 ± 0.4 nm, nearly identical to that found in pure DMPC.

3.2.2. Time-Dependent Studies. To understand the differences between images of the PMA-free and PMA-modified bilayers, we examined the time dependence of the AFM images. Of particular interest were the dynamics of the island features within the defects. Figure 4 shows sequential images following those shown in Figure 3 when the bilayer surfaces were continuously imaged for extended times. Figure 4a shows time-dependent images obtained from the DMPC bilayer absent PMA. Figure 4a shows that after 2 min at 13 °C, the shape of the defect features had changed. Lipid globules had diffused toward the edges of the defects, fusing into larger patches of lipids. After another 3 min, Figure 4b reveals that the number of isolated lipid islands was significantly reduced compared to the initial state in Figure 3a. This phenomenon has been previously observed in many AFM studies.[12,31−33] The island coalescence occurred in a manner akin to Ostwald ripening. Small islands coalesced to larger patches, resulting in a reduced perimeter to surface area ratio. Figure 4a,b reveals that even though the lipids were in a rigid gel phase at this temperature, nonetheless they possessed the capacity to diffuse in order to minimize their surface energy.

Time-dependent images of the DMPC−PMA system are shown in Figure 4c,d. In contrast to the PMA-free system,

(30) Giocondi, M.-C.; Pacheco, L.; Milhiet, P. E.; Grimellec, C. L. *Ultramicroscopy* **2001**, *86*, 151−157.
(31) Muresan, A. S.; Lee, K. Y. C. *J. Phys. Chem. B* **2001**, *105*, 852−855.
(32) Leonenko, Z. V.; Carnini, A.; Cramb, D. T. *Biochim. Biophys. Acta* **2000**, *2000*, 131−147.
(33) Reviakine, I.; Brisson, A. *Langmuir* **2000**, *16*, 1806−1815.

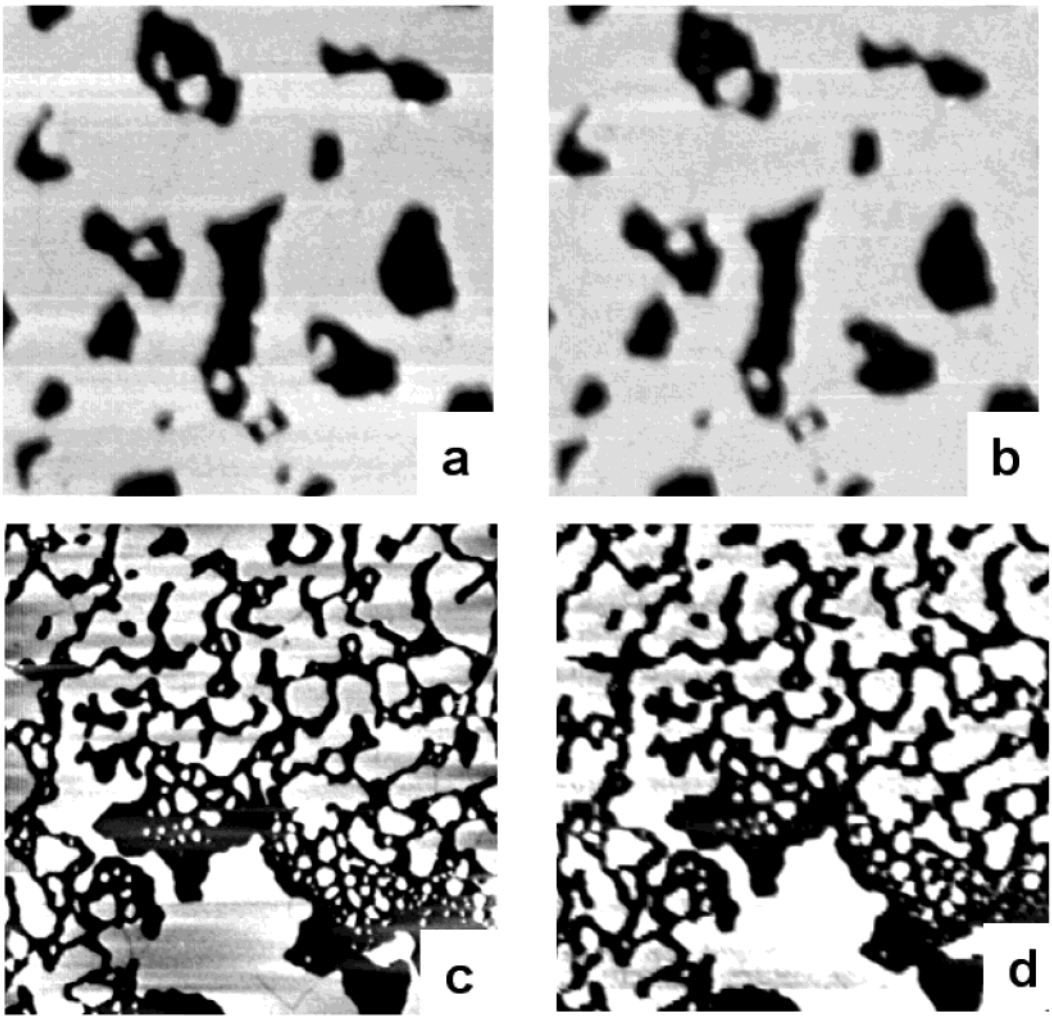

Figure 4. MAC-mode AFM images from pure DMPC bilayers (a,b) (3 × 3 μm) and DMPC + PMA (c,d) (5 × 5 μm) on mica at 13 °C: (a) $t = 2$ min and (b) $t = 5$ min after Figure 3a; (c) $t = 2$ min and (d) $t = 7$ min after Figure 3b. Dark color is the mica substrate, and light color is the lipid bilayer.

images of the polymer-modified system were nearly time-invariant, especially in terms of the position and the wide size distribution of the islands. Even after 7 minutes, no significant changes are observed as seen in Figure 4d.

3.2.3. Temperature Dependence. Figure 5 examines the temperature dependence of AFM images from bilayers with and without added PMA at temperatures below and just before the phase transition temperature. Figure 5a−c shows AFM images obtained from the pure DMPC bilayer at various temperatures below the main phase transition temperature. Since the sample was equilibrated at each temperature for 3−5 min, this sequence of images was captured over 15 min. Initially, at 14 °C, small irregular-shaped defects incorporating lipid islands were observed as described previously. As the temperature increased, Figure 5b obtained at 20 °C shows that considerable change to the defects had occurred. In particular, substantial lipid island diffusion was evident (circled area) and in addition one observes significant changes in the shape of the defects (squared area). Figure 5c, showing a nearby area at 22 °C, evinces further changes in morphology just before the phase transition. This image shows the appearance of fine lines connecting the defects and the appearance of other small defects that are associated with the start of the phase transition. These features have been observed previously.[12,14] The depth of the fine line features was not possible to obtain quantitatively, due to the finite size of the AFM tip. The changes in images a−c are results of the combined effects of lipid diffusion and annealing of defects prior to the lipid phase transition.

Upon addition of PMA to the phospholipid bilayer system, large defected areas with small lipid islands were observed as shown in Figure 5d, which was obtained at 14 °C. Due to a slight temperature drift during this experiment, Figure 5e drifted slightly from Figure 5d. The black arrows in Figure 5d,e identify the same features. Figure 5e obtained at 20 °C exhibits features that closely resemble those found at the lower temperature. The shape and size of the lipid islands remain unchanged within defects. The major difference between Figure 5d and Figure 5e is the appearance of thin channels connecting small defects within the large lipid patch at the higher temperature. These lines are similar to those observed in Figure 5c observed at 22 °C in the pure DMPC bilayer but are observed at some 2 °C lower temperature in the presence of PMA. The lines are approximately 60−80 nm wide and 1−1.5 nm deep. When the temperature is increased further to 21 °C, Figure 5f (obtained in an adjacent area) shows more of these lines. Images obtained above 30 °C (in the lipid fluid phase) exhibit morphological invariance with or without PMA (data not shown). At this temperature, all defects were filled with lipid and the surface exhibited a homogeneously flat morphology as described previously.[12]

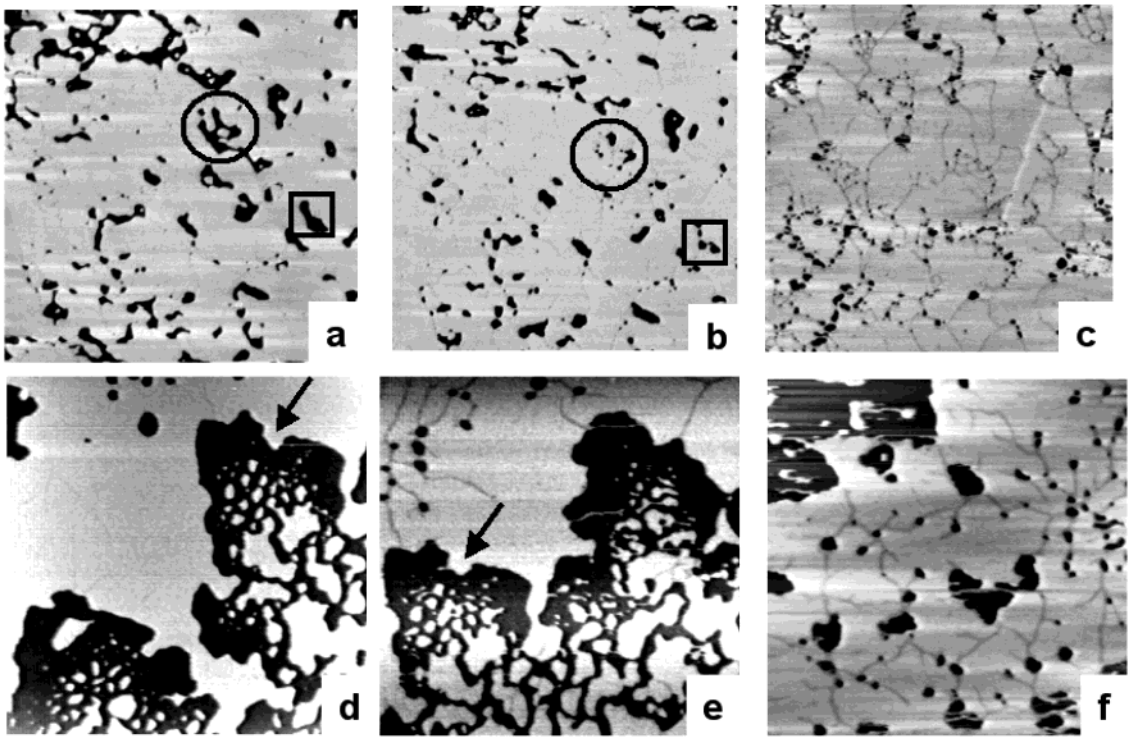

Figure 5. MAC-mode AFM images from pure DMPC bilayers (a−c) and DMPC + PMA (d−f) on mica at various temperatures: (a,d) $T = 14$ °C, (b,e) $T = 20$ °C, (c) $T = 22$ °C, and (f) $T = 21$ °C. Images are all 5×5 μm. Dark color is the mica substrate, and light color is the lipid bilayer.

4. Discussion

The results presented above provide considerable insight into the changes wrought by the adsorption of the polyelectrolyte (PMA) to the supported DMPC bilayer in its gel phase. In particular, we discuss the change in phase transition temperature and cooperativity of the lipid and changes in the defects formed. Finally, we provide a model for the interaction of PMA with DMPC bilayers.

4.1. Decreased T_m. Figure 2c shows a shift of the main phase transition temperature, T_m, from 23.5 to 21.4 °C when PMA is added to the DMPC bilayer system. To our knowledge, this is the first time that changes in T_m induced by the addition of macromolecules to a supported lipid bilayer have been observed. However, several research groups have reported calorimetric results from multilamellar or unilamellar vesicles when polymers[1,16,34,35] or peptides[36−38] were added. The decrease in T_m shows that polymer destabilizes the gel phase of the bilayer, perhaps by interfering with the lipid packing needed to form the gel phase.

Looking more quantitatively at these data, we note that when the polymer was added to the DMPC bilayer, a slight asymmetry was observed in the dL/dT plot shown in Figure 2c. In measurements utilizing calorimetry, a shoulder at the lower temperature end of the heat capacity profile is taken to indicate unfavorable partitioning of the solute molecules into the gel phase.[37] Since the L value is used to monitor the phase transition in a way analogous to that provided by heat, the asymmetry observed in our ellipsometry results upon PMA addition supports the slightly higher affinity of PMA to the fluidlike surfaces.

These conclusions obtained from ellipsometry are supported by the AFM images. These images show that the strain-induced crack and defect formation that we found previously to be a precursor to the phase transition occurs at some 2 °C lower temperature in the presence of PMA. That cracking and defect formation occur both with and without PMA suggests that the phase transition occurs in the same manner upon addition of polymer. However, we note that the PMA-modified bilayer is substantially more defected than that absent PMA and that the defect annealing process below T_m is diminished when the polymer is present (vide infra). This means that the filling of defects must occur during the course of the phase transition, which provides a phenomenological explanation for the increased width of the transition found in the dL/dT plot. We give a more quantitative explanation for this width in the next section.

4.2. Cooperative Unit, N, from Ellipsometry Curves. The ellipsometry curve shows a sharp change in thickness at T_m. Since AFM measurements indicate that gel and fluid phases coexist around T_m, we used the proportional thickness as determined by the ellipsometry to obtain the fraction of lipid in each phase as a function of temperature, T. The natural log of the ratio of the fraction of lipid in the gel and fluid phases was plotted against $1/T$ within the range of phase transition (data not shown). The slope of a linear fit to this plot gives the van't Hoff enthalpy for the phase transition.[12] Taking the enthalpy for phase transition of DMPC single bilayer vesicles to be $\Delta H_t = 2.25 \times 10^4$ J/mol,[39] the cooperative units for the phase transition with and without PMA were

(34) Schroeder, U. K. O.; Tirrell, D. A. *Macromolecules* **1989**, *22*, 765−769.
(35) Yoshida, A.; Yamauchi, H.; Sakai, H.; Kawashima, N.; Abe, M. *Colloids Surf., B* **1997**, *8*, 333−342.
(36) Epand, R. M.; Sturtevant, J. M. *Biophys. Chem.* **1984**, *19*, 355−362.
(37) Ivanova, V. P.; Makarov, I. M.; Schaffer, T. E.; Heimburg, T. *Biophys. J.* **2003**, *84*, 2427−2439.
(38) Prenner, E. J.; Lewis, R. N. A. H.; Kondejewski, L. H.; Hodges, R. S.; McElhaney, R. N. *Biochim. Biophys. Acta* **1999**, *1417*, 211−223.
(39) Mabrey, S.; Sturtevant, J. M. *Proc. Natl. Acad. Sci. U.S.A.* **1976**, *73*, 3862.

determined to be $N = \Delta H_{vH}/\Delta H_t$. The cooperative units are determined to be 114−156 and 16−20 for pure DMPC and DMPC−PMA, respectively. This number for the pure DMPC bilayer cooperativity is 3-fold higher than the previous measurement from a supported single bilayer from AFM images[12] and 4 times smaller than that determined from multibilayer dispersions of DMPC measured by light scattering.[27] One possibility for the difference might be the use, in the present experiments, of a different solid support (mica rather than SiO_2). A slight difference in diffusion coefficient has been suggested for lipid spreading over mica and SiO_2.[40,41]

The addition of PMA introduces an almost 10-fold decrease in cooperativity of the phase transition for the supported lipid bilayer. This decrease suggests strong PMA interaction with the bilayer and modification of bilayer physical properties, as also suggested from FTIR results.[15] The decreased cooperativity of the transition with PMA may stem from two reasons. First, as observed from AFM images, lipid islands were significantly smaller; upon adding PMA, the lipid islands decrease in size by a factor of 3−4. These smaller islands may limit communication between regions of lipids during the phase transition. Second, since from common sense it is expected that the hydrophobic core of the membrane is sheltered from the aqueous environment, the edges of lipid disks most likely possessed higher surface curvature. Smaller lipid islands imply a large population of such curved lipids. The effect of the modified radius of curvature of the lipid patches may disrupt the close packing of the lipid molecules and limit the range of the cooperative interaction.

4.3. Small Islands and Uniform Cracking in the Presence of PMA. A striking feature of the AFM images when PMA was present is the significantly smaller size of the lipid islands and the uniformly divided larger lipid patches in the highly defected areas. In Figures 3b and 4c,d, the line-shaped defects branch from the edges of the defects at the lower part of the images upward to divide the lipid into patches. The line widths of the channels were remarkably uniform. As already noted above, a random selection of 10 channels gave a line width of 148 ± 30 nm. The formation of such small lipid islands and relatively evenly divided patches most likely results from immobilization of the gel-phase lipid by PMA. Recall the history of these experiments: PMA was incubated with the preformed lipid bilayer above 30 °C, followed by rapid cooling back to the gel phase during sample preparation. As the gel phase formed, the lipid bilayer surely experienced lateral contraction, leading to cracking of the bilayer film.[12] Normally, without the presence of PMA, lipid islands diffuse to minimize their surface energy by coalescence into nearby patches, as shown in Figures 3a and 4b,c. However, because of the suppressed diffusion of the lipid bilayer by PMA, lipid islands and patches remained isolated. The resulting highly uniform defect channels clearly indicate that the contraction during the lipid phase transition occurred uniformly over the bilayer surface.

4.4. Diffusion of Lipid Islands in Defects Absent PMA. Results from our AFM experiments show that the gel-phase lipid bilayer was mobile on the mica support, although less mobile than in the fluid phase. As a function of either time or temperature, the defect morphology changes in the pure DMPC bilayer when small islands of DMPC move to the island edges and are incorporated. The highly dynamic nature of lipid molecules on hydrophilic solid supports has been discussed extensively in prior literature.[12,31−33,42]

Two lipid islands in Figure 3a are labeled with white arrows to indicate their motion toward the lipid walls. One of them diffused upward (labeled I), and the other to the lower-left side (II). Thus, the motion of the islands was not always directed toward the closest defect edge. Rather, the islands appeared to move randomly within the defect until an edge was reached. Lipid islands experience higher line tension because they require additional energy to curve the lipid molecules at the edge to prevent exposure of the hydrophobic core of the bilayer to the aqueous environment.[31] Therefore, once a lipid island hits the lipid wall, it fuses into the larger patch to minimize the perimeter to surface area ratio. The growth of larger patches of lipid at the expense of smaller lipid islands via diffusion is analogous to two-dimensional Ostwald ripening. However, we emphasize that the mechanism of this annealing process occurs via diffusion of the entire island rather than desorption of individual lipid molecules from the smaller patch and their reattachment to the larger one.

Assuming linear (uniform) movement of the lipid islands, these time-dependent images reveal the lipid island diffusion rate within the bilayer defects. Analysis of the island−lipid wall distance gives a mean lipid velocity ranging between 0.05 and 1.30 nm/s with larger islands traveling more slowly. This is consistent with the previously reported longer relaxation time required for larger bilayer patches.[31] This may also explain why large lipid patches appear immobile in the time scale of our AFM study. Within the linear approximation used to obtain these velocities, these coefficients reveal a fairly slow velocity of the free-standing gel-phase lipid islands within defects on the mica surface. By way of comparison, the diffusion coefficient for individual lipid molecules within a bilayer is reported to be 7×10^{-11} cm^2/s for gel-phase DMPC at 16 °C,[43] giving a root-mean-square (rms) displacement of 118 nm in 1 s. The rates we measure are 2 orders of magnitude smaller.

This encourages one to inquire into the origins of island motion. There are two issues here. Regarding mechanism, prior studies of bilayer spreading suggest two possibilities.[40,44,45] First, the bilayer might move by sliding atop the water layer between it and the mica surface. Second, the bilayer can move via an internal rolling process wherein the top layer moves relative to the bottom. Furthermore, one can inquire into the driving force behind this motion. That lipid islands move randomly in various directions eliminates the possibility that AFM tip and lipid sample interaction might be the cause of lipid movement. Instead of lipid spreading in the same direction, the lipid islands in our AFM images appear to exhibit a random walk due to fluctuations. This driving force is different from that presented by studies involving a reservoir of unfused lipid on the surface.[40,44,45]

4.5. Suppressed Diffusion of Lipid with PMA. Addition of PMA to the bilayer islands suppresses island mobility. Quantification of this process is given in Figure

(40) Radler, J.; Strey, H.; Sackmann, E. *Langmuir* **1995**, *11*, 4539−4548.
(41) Tamm, L. K. *Biochemistry* **1988**, *27*, 1450−1457.
(42) Evert, L. L.; Leckband, D.; Israelachvili, J. N. *Langmuir* **1994**, *10*, 303−315.
(43) Marsh, D. *Handbook of lipid bilayers*; CRC Press: Boca Raton, FL, 1990.
(44) Nissen, J.; Gritsch, S.; Wiegand, G.; Radler, J. O. *Eur. Phys. J. B* **1999**, *10*, 335−344.
(45) Nissen, J.; Jacobs, K.; Radler, J. O. *Phys. Rev. Lett.* **2001**, *86*, 1904−1907.

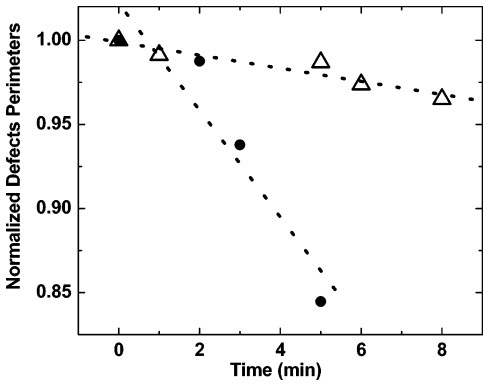

Figure 6. Time-dependent changes in defect perimeters of the pure DMPC bilayer (circles) and of DMPC + PMA bilayers (triangles) at 13 °C. Each data point is obtained from measurement of an AFM image.

6, showing the normalized defect perimeters plotted as a function of time. Figure 6 compares the rate of normalized perimeter change with and without PMA incorporated into the DMPC bilayer. The plots were fitted linearly to obtain numerical values for the perimeter-changing rate for each case depicted in Figures 4 and 5. The circular and open triangular symbols describe the DMPC lipid bilayer at a constant temperature (13 °C) without and with PMA adsorption, respectively. Linear fits to both plots give slopes of 0.032 and 0.0039 min^{-1}. This shows a more than 8-fold decrease in the suppressed perimeter-changing rate (dP/dt) upon PMA adsorption.

4.6. Effect of PMA Adsorption on the DMPC Bilayer. We now discuss tentatively ways in which PMA might adsorb on the DMPC bilayer and ways in which this adsorption might hinder lipid diffusion on the surface. There are three general ways in which a polymer may interact with lipid membranes: (i) adsorption, (ii) insertion into the bilayer, and (iii) complete disruption of the bilayer, with formation of mixed polymer−lipid micelles or other aggregates. Our AFM and ellipsometry results strongly argue against the latter. Furthermore, in previous work we showed that PMA neither penetrates into the hydrophobic core of the bilayer nor penetrates to the underlying substrate.[15] Having discarded the alternative possibilities, we conclude that the polymer associated with the outermost headgroup region of the lipid bilayer. We note that while a single polymer chain has been imaged on mica in air using AFM,[46] the observed height was small (0.1−0.2 nm) and may not be resolvable on the somewhat more heterogeneous gel-phase bilayer film.

Headgroup association of the polymer with the lipid bilayer is supported by results presented here. Ellipsometry measurements showed that the lipid bilayer thickness decreases slightly (0.25 nm) upon PMA adsorption. This slight decrease is consistent with a change in headgroup tilt from 46.6° to 56.9°, known from IR measurements to occur upon polymer adsorption.[15] However, the highly stabilized defect edges in our AFM images lead us to speculate that the polymer favors defect edges over flat lipid patches for adsorption sites. As noted above, defect edges are aligned by hemispherical micellar-shaped lipid molecules to avoid the exposure of the hydrophobic interior of the bilayer to the aqueous environment. Such sites are less densely packed and more disordered than for a flat bilayer membrane surface. Since our ellipsometry results have clearly demonstrated the preferred interaction of

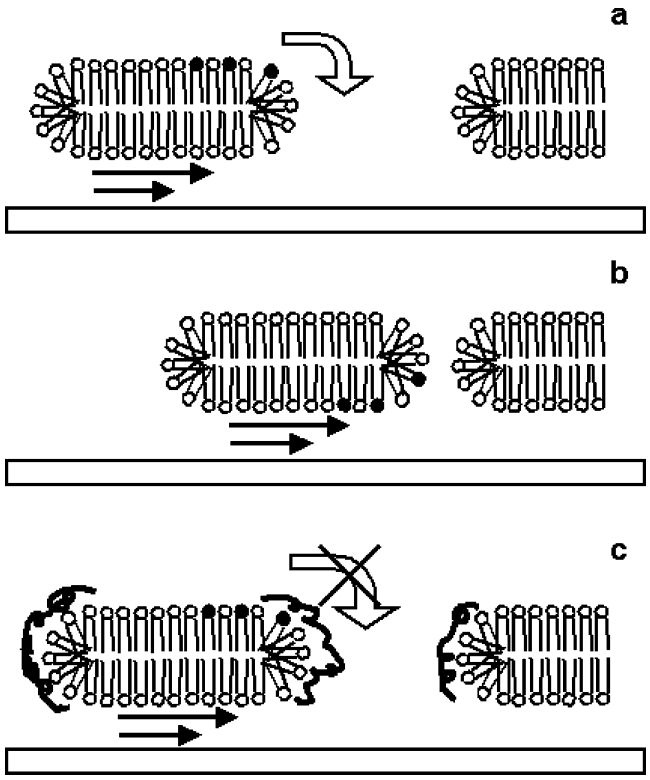

Figure 7. Schematics of a suggested model of lipid island diffusion upon PMA adsorption: (a) lipid island, defect, and large patch of lipid; (b) the island diffuses by internal rolling and sliding toward the lipid patch when free of PMA; (c) PMA adsorption at the edge of the lipid, hindering the internal rolling process. Black circles represent the headgroup of any three lipid molecules.

PMA with more disordered and less densely packed fluid-phase lipid membrane, we suggest that PMA is more likely to adsorb to the defect edge sites than to the patch membrane surface. This conjecture was anticipated in an earlier study of a similar polymer (poly(2-ethylacrylic acid), PEAA) stabilizing the inner surface of the pores of lipid vesicles.[47]

This conjecture is reasonable when one compares the number of lipid molecules influenced by polymer adsorption to the number of lipid molecules at edge sites. Given the AFM cell size of 1.27 cm^2 and the lipid thickness of 4.4 nm, taking the headgroup of fluid-phase lipids to be 63 $Å^2$ and that of the gel-phase lipid to be 45 $Å^2$,[30] the percentage of lipid at the edge sites is 4.5% of the total number of lipids. This number is slightly smaller than the 5% of total adsorption percentage of PMA controlled by contact time and therefore shows that there was sufficient PMA in the system to fully cover the edge sites of the lipid membrane to stabilize the defect edges.

Considering further this tentative model in which polymer preferentially associates with the lipids at defect edges, we now address the decrease in mobility after adsorption. As mentioned previously, bilayer mobility in the circumstances considered here can occur via either a sliding or rolling mechanism. Although our study does not differentiate between these possible mechanisms, we conjecture that the preferential adsorption on edge lipids creates heterogeneity on a lipid globule. Therefore, a rolling mechanism is unlikely to happen upon polymer adsorption. Furthermore, it is reasonable to suppose that

(46) Kumaki, J.; Nishikawa, Y.; Hashimoto, T. *J. Am. Chem. Soc.* **1996**, *118*, 3321−3322.

(47) Chung, J. C.; Gross, D. J.; Thomas, J. L.; Tirrell, D. A.; Opsahl-Ong, L. R. *Macromolecules* **1996**, *29*, 4636−4641.

PMA adsorption stabilizes discrete surface structures by reducing the line tension experienced by the lipids at defect edges. Therefore, lipid mobility is hindered by PMA. With these thoughts in mind, we tentatively propose the following model. Figure 7 shows a possible model of PMA interaction with the DMPC bilayer membrane. Figure 7a,b shows a free lipid island, diffusing by a combination of sliding and rolling toward a nearby lipid patch site. Figure 7c shows the PMA adsorbs on the free edge of the defect, which hinders the rolling mechanism.

5. Prospects

Looking to the future, these measurements have a bearing on understanding the binding of polymers to lipid membranes, which is a subject of interest not just from biological and biophysical standpoints but also in formulating sensors and many cosmetics and pharmaceutical products. The systematic, regular, quantitative patterns of behavior reported here show that these lipid membranes constitute responsive surfaces that differ strongly from polymer adsorption onto traditional "hard" surfaces. Not yet clearly understood is the degree to which the long defect equilibration times in the gel phase, reported in the present study, may be related to the slow changes in headgroup orientation that we observed previously using infrared spectroscopy in both the gel and fluid phases.[15]

Acknowledgment. We are indebted to Adelé Poynor for assistance with the ellipsometry measurements and to Liangfang Zhang for assistance in methods to form supported fluid bilayers. Z.V.F. acknowledges the Department of Chemistry for financial support in the form of the Lester E. and Kathleen A. Coleman Fellowship. This work was supported by the U.S. Department of Energy, Division of Materials Science, under Award No. DEFG02-91ER45439 through the Frederick Seitz Materials Research Laboratory at the University of Illinois at Urbana−Champaign.

LA049030W